http://www.press.ierek.com

ISSN (Print: 2357-0849, online: 2357-0857)

Environmental Science and Sustainable Development

Research Paper

Received:07 October 2025, Accepted: 21 December 2025, Published online: 31 December 2025

DOI: 10.21625/essd.v10i4.1250

Performance enhancement of microbial fuel cells through g-C_3N_4-embedded biochar anodes

Tsuyoshi Arao[a], Trang Nakamoto[b], Kozo Taguchi[c]

[a] *Master student of Electronic Systems at Ritsumeikan University, Kusatsu, Shiga, Japan*

[b] *Assistant Professor of R-GIRO, Ritsumeikan University, Kusatsu, Shiga, Japan*

[c] *Professor of the College of Science and Engineering, Ritsumeikan University, Kusatsu, Shiga, Japan*

Abstract

Global demand for sustainable energy technologies capable of simultaneously generating electricity and treating wastewater has intensified interest in microbial fuel cells (MFCs). However, their practical application remains limited by low power density and insufficient electron-transfer efficiency at the anode. This study addresses this challenge by embedding graphitic carbon nitride (g-C_3N_4), a metal-free and environmentally benign material, into rice-husk-derived biochar to develop a low-cost, sustainable anode. Unlike conventional surface-coated electrodes, the embedded configuration enhances internal electron-transfer pathways and promotes microbial colonization throughout the electrode matrix. Anodes with 5, 10, and 12 wt% g-C_3N_4 were evaluated to clarify how nitrogen-rich functional groups and carbon conductivity interact to influence MFC performance. The 5 wt% anode exhibited the most favorable electrochemical behavior, achieving a maximum power density of 43.245 μW/cm² —approximately 1.9 times higher than the unmodified anode—highlighting the effectiveness of moderate nitrogen incorporation. Excessive loading reduced performance due to impaired conductivity. These findings provide new insight into the design of sustainable, biomass-derived anode materials and demonstrate the potential of g-C_3N_4-embedded biochar for scalable, environmentally friendly MFC applications. This work contributes to the global scientific effort toward low-cost, renewable energy systems for wastewater treatment and decentralized power generation.

Keywords

Microbial Fuel Cell; Graphitic Carbon Nitride; Biochar Anode; Floating Cathode; Sustainable Energy

1. Introduction

In recent years, rapid technological innovation and global population growth have led to a dramatic increase in global energy demand and freshwater consumption. Under these circumstances, dependence on fossil fuels as conventional energy sources has resulted in serious environmental impacts such as CO_2 emissions, resource depletion, and water contamination, creating a major barrier to achieving a sustainable society. To address these issues, the development of renewable and environmentally compatible energy systems is urgently required.

Microbial fuel cells (MFCs) have attracted increasing attention as a bioelectrochemical technology capable of simultaneously treating wastewater and generating electricity by utilizing electrogenic microorganisms as biocatalysts (Pant et al., 2010; Sayed et al., 2020). In MFCs, electrogenic microorganisms oxidize organic substrates at the anode,

releasing electrons, protons, and carbon dioxide. (Pant, D. et al., 2010). These electrons travel through an external circuit to the cathode, where they react with oxygen to form water, enabling both wastewater purification and power generation (Sayed, E.T. et al., 2017). However, low power output remains one of the most critical challenges limiting the practical application of MFCs. Improving electron-transfer efficiency and optimizing anode materials are essential for achieving stable, high-performance operation. Because the anode directly mediates electron transfer and strongly influences biofilm development, its material properties and surface chemistry are pivotal to overall MFC performance.

To overcome these limitations, this study focuses on graphitic carbon nitride (g-C_3N_4), an environmentally friendly and easily synthesized metal-free catalyst that has recently gained attention for its nitrogen-rich functional groups and stability (Mishra, A. et al., 2018; 2019). While previous research has mainly improved anode performance by coating g-C_3N_4 onto carbon surfaces (Jian, M. et al., 2024; Sayed, E.T. et al., 2021), such surface-only modification may not fully enhance internal electron transport or microbial activity throughout the porous structure. Moreover, the influence of g-C_3N_4 distribution within biochar materials and its effect on the balance between conductivity and biofilm formation has not been sufficiently examined. While prior studies have investigated the benefits of carbon-based anode modifications, the specific role of g-C_3N_4 within the anode matrix and how its distribution interacts with microbial and electrochemical processes remains underexplored. This study fills this gap by providing comparative insight into these interrelated mechanisms.

The main contribution of this work is to systematically evaluate how different amounts of *g-C_3N_4* incorporation influence biofilm development and electron-transfer behavior in biochar-based anodes. The results demonstrate that 5 wt% provides the optimal balance by enhancing microbial colonization and maintaining sufficient conductivity. Furthermore, embedding within the biochar matrix, rather than coating it only on the surface, offers new insight into forming internal electron-transfer pathways that improve overall MFC performance.

2. Materials and Methods

2.1. Synthesis of g-C_3N_4

Synthesis of g-C_3N_4 was performed by conventional methods (Yan S. C. et al.,2009). Melamine was purchased from Wako Pure Chemical Industries. To ensure reproducibility, the heating program was carefully controlled to prevent premature decomposition and promote polymerization of melamine into g-C_3N_4. The sample was placed in a crucible and sealed with a lid to prevent sublimation. First, the sample was heated to 500°C at a heating rate of 20°C/min and held for 2 hours. Then, the heating rate was changed to 5°C/min, and the sample was heated to 520°C and held for 2 hours. After the heat treatment, the sample was cooled naturally to room temperature, and the resulting solid was powdered using a mortar. Figure 1 shows the scanning electron microscopy (SEM) image of the synthesized g-C_3N_4 powder. The synthesized particles ranged in size from approximately 10 to 40μm

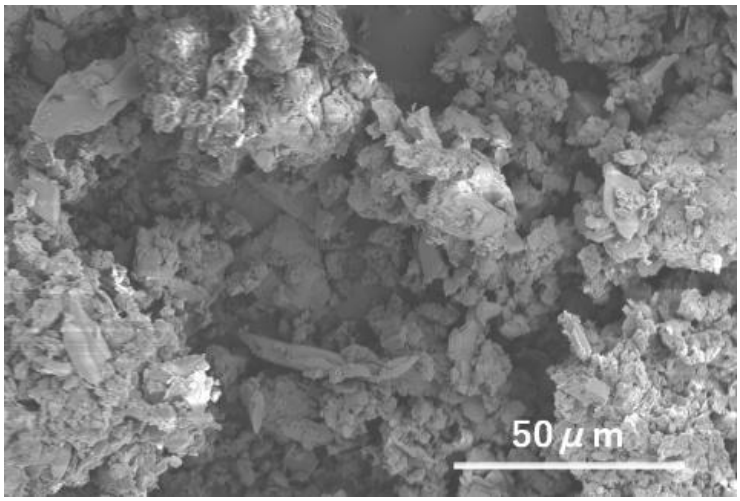

Figure 1: SEM image of g-C_3N_4.(source: by authors)

2.2. Electrode Preparation

Rice-husk-derived carbon (RHC) was selected for its porous structure, high surface area, and low production cost, making it suitable for microbial colonization. The RHC was subjected to alkaline etching by stirring in a 6 mM sodium hydroxide solution at 90°C for 24 hours. After treatment, the mixture was carefully rinsed with deionized water and then air-dried at 60 °C for 12 hours. The resulting material was then ground into a fine powder using a mortar and pestle.

Electrode fabrication was carried out according to the method described in (Hirose, S. et al. 2023). For the cathode, a mixture consisting of Co–MnO_2 catalyst (0.75 g), RHC (0.525 g), and carbon ink (3 mL of commercial sumi ink) was prepared and used as the catalyst layer. For the anode, a mixture of RHC (0.9 g) and sumi ink (3.5 mL) was homogenized and cast into a 2 cm × 2 cm mold fabricated by 3D printing. A stainless steel mesh was embedded into the mixture, and the electrode was air-dried at 60°C for 24 hours.

To incorporate graphitic carbon nitride (g-C_3N_4) into the anode material, the powdered RHC was modified by dispersing 5 wt%, 10 wt%, and 12 wt% g-C_3N_4 in methanol and then stirring for 24 hours. After dispersion, the solid was collected via centrifugation and dried at 60°C for 24 hours to obtain g-C_3N_4-modified RHC. The resulting modified carbon material was then mixed with sumi ink and used to fabricate the g-C_3N_4-containing anode electrodes.

2.3. Preparation of Culture Medium

Luria-Bertani (LB) medium was utilized as the nutrient source for microbial cultivation. The medium was prepared by dissolving 5.0 g of tryptone, 2.5 g of yeast extract, and 5.0 g of sodium chloride (NaCl) in 380–400 mL of deionized water, ensuring that the total volume would not exceed 400 mL after all components were added. Separately, 0.5 g of sodium hydroxide was dissolved in 40 mL of deionized water, and 2.5 mL of this solution was added to the primary mixture. If the total volume was still below 400 mL at this stage, deionized water was added to bring it to 400 mL. Subsequently, an additional 100 mL of deionized water was added, and the final mixture was sterilized by autoclaving to complete the preparation of LB medium.

2.4. Configuration of the MFC

The microbial fuel cell (MFC) employed in this study was constructed as a single-chamber system equipped with a floating air cathode, as illustrated in Figure 2. In this system, the anode and cathode coexist in the same chamber, simplifying the structure and improving ease of operation. The chamber was filled with a reaction solution composed of 100 mL of Luria-Bertani (LB) medium as a nutrient medium and 500 mL of water for dilution. Mud collected from the natural environment in Japan was used as the microbial source, of which 2.5 mL was added to the reaction system.

Compared with the double-chamber type, the single-chamber MFC has a simpler structure and does not require an intermediate ion-exchange membrane, thereby reducing manufacturing costs and internal resistance. In addition, since oxygen from the air can be supplied directly to the cathode (Li, W.-W. et al., 2011) (Logan, B. E. et al.,2006), it does not require an external energy supply and has excellent operational efficiency and scalability, making it a promising configuration for practical use.

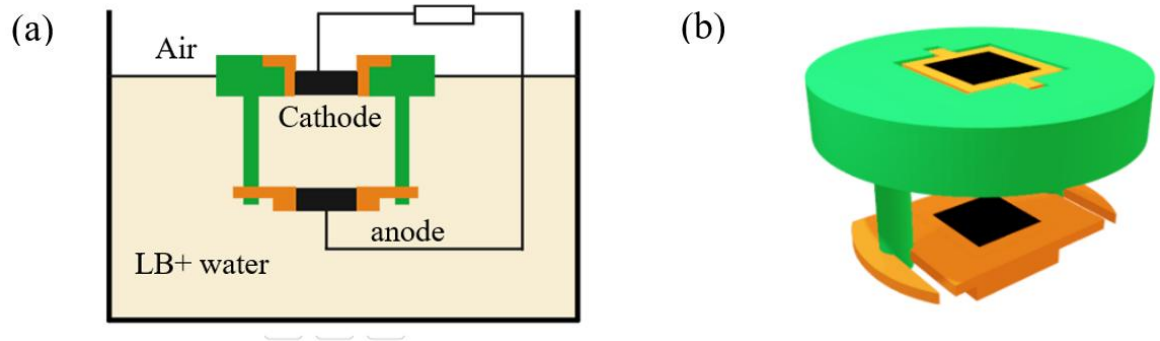

Figure 2: (a) Schematic diagram of a single-chamber microbial fuel cell with a floating air cathode. (b) Float model diagram.(source: by authors)

2.5. Evaluation of MFC operation

A fixed 10 kΩ external resistor was continuously connected between the anode and cathode of the MFC throughout the experiment to ensure a stable discharge condition. Experiments were performed under controlled ambient conditions at 25 ± 1 °C. Daily fluctuations in solution level caused by evaporation were compensated for by replenishing with tap water as needed. Electrode potential and power density were used as indicators of performance. The external resistance varied in steps from 10,000 Ω to 200 Ω, and the voltage at both ends at each resistance value was measured. From these voltage values and the corresponding resistance values, the current and power were calculated and further divided by the effective surface area of the anode to obtain the current density and power density. In addition, power density measurements were performed multiple times during the experimental period to evaluate changes in the power generation characteristics of the MFC over time. Ag/AgCl electrodes were employed as reference electrodes to measure the electrode potentials. The power generation voltage (V) of the MFC was defined as the potential difference between the anode and the cathode, and is represented by the following equation.

$$V = E_{cathode} - E_{anode} \qquad (1)$$

The voltage applied to the external resistors was measured using a data acquisition device (DAQ) controlled by LabVIEW, which automatically recorded voltage data at 15-minute intervals.

2.6. g-C_3N_4 evaluation

To investigate whether g-C_3N_4 was successfully incorporated and supported on the rice husk biochar, the elemental composition of the particles was analyzed using Energy Dispersive X-ray Spectroscopy (EDS).

3. Experimental Results

3.1. Composition of g-C_3N_4-Modified Biochar

Figures. 3 and 4 provide a comprehensive visualization of the structural and elemental characteristics of biochar modified with 10 wt% g-C_3N_4. Figure 3(a) presents the SEM image of g-C_3N_4-modified biochar, illustrating its surface morphology. Figure 3(b), (c), (d), and (e) show the elemental mapping images of carbon (C), nitrogen (N), oxygen (O), and silicon (Si), illustrating their respective spatial distributions and providing evidence for the successful incorporation of g-C_3N_4 into the biochar structure.

Figure 4 shows the corresponding EDS spectrum of the modified biochar; the X-axis corresponds to the energy of the X-rays, while the Y-axis indicates the signal intensity. The mass percentages of detected elements are summarized in Table 1. The measured elemental composition consisted of carbon (80.83%), nitrogen (6.41%), oxygen (10.93%), and silicon (1.83%).

In contrast, the EDS results for the unmodified biochar, shown in Table 2, indicate the absence of nitrogen. These data clearly demonstrate that g-C_3N_4 was successfully incorporated into the biochar using the experimental method employed in this study.

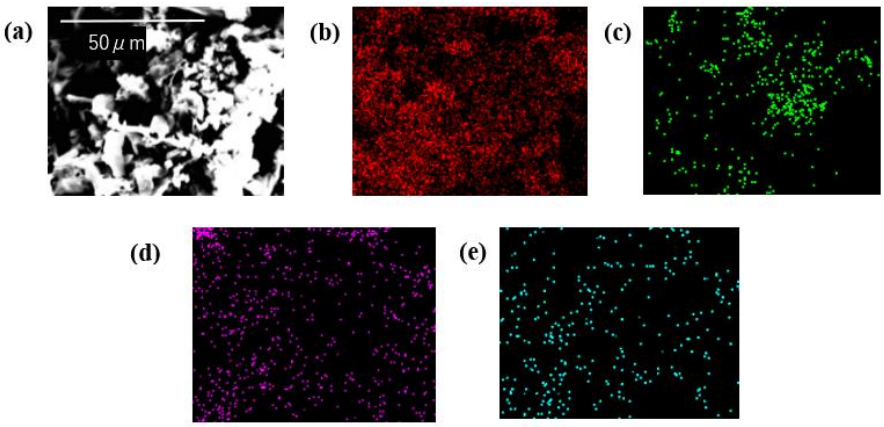

Figure 3: Morphology and elemental mapping of biochar modified with 10 % g-C_3N_4. (a) SEM micrograph, and (b) carbon (C), (c) nitrogen (N), (d) oxygen (O), (e) silicon (Si) mapping. (source: by authors)

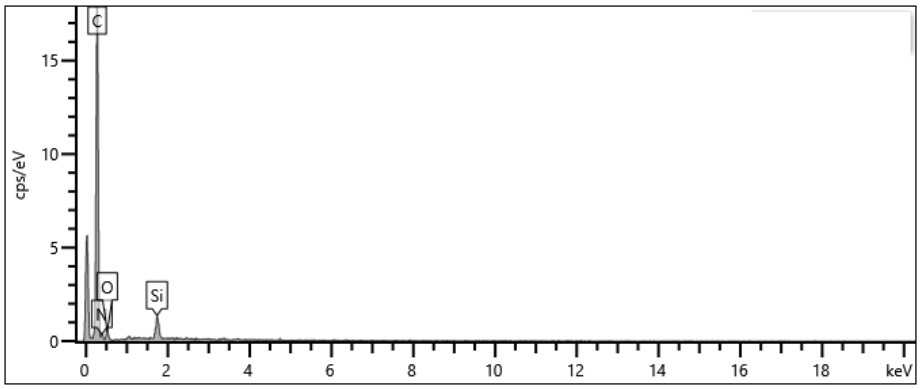

Figure 4 EDS spectrum of biochar modified with 10 wt% g-C_3N_4.(source: by authors)

Table 1. Elemental composition of g-C_3N_4-modified biochar

Chemical element	Mass (%)
C	80.83
N	6.41
O	10.93
Si	1.83
total	100.00

Table 2. Elemental composition of unmodified biochar

Chemical element	Mass (%)
C	86.04
N	0.00
O	12.51
Si	1.45
total	100.00

3.2. Evaluation of the impact of g-C_3N_4 mixed anodes

Figure 5 illustrates the temporal evolution of anode potentials relative to the Ag/AgCl reference, demonstrating the effect of g-C_3N_4 incorporation into the anode material under the same cathode conditions. By keeping the cathode conditions constant, the changes observed are attributed to the anode configuration, as the potential was maintained. Focusing on the anode potential, the anode with 5 wt% g-C_3N_4 had the highest potential at -540 mV at 14 days, higher than the other conditions. The more negative anode potential observed in the 5 wt% electrode indicates greater electron-accepting capability, suggesting improved microbial electron-transfer kinetics. This trend aligns with reports that nitrogen-rich materials facilitate microbial adhesion and redox activity. However, since g-C_3N_4 is not intrinsically highly conductive, increasing the loading to 10 wt% or 12 wt% diminished the electrochemical performance. This suggests that the addition of g-C_3N_4 improves anodic performance only in the appropriate concentration range, beyond which the balance between conductivity and microbial activity may become unbalanced and counterproductive.

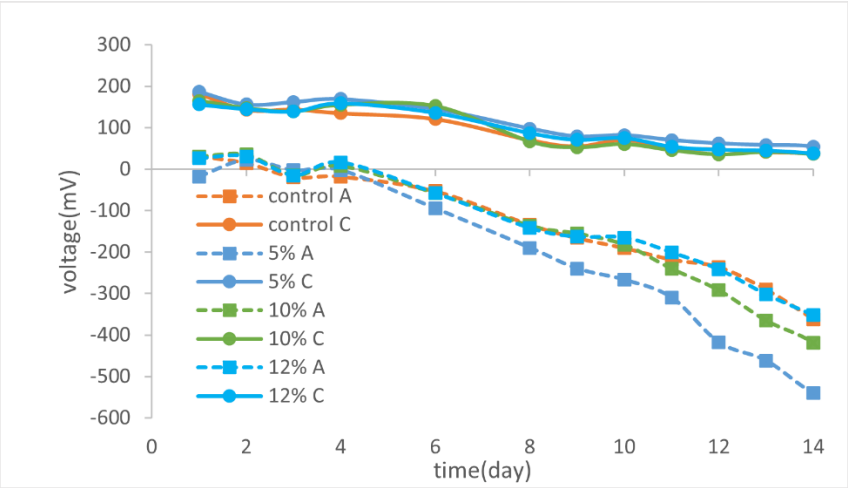

Figure 5 Evolution of Ag/AgCl potentials in MFCs using biochar anodes with different g-C_3N_4 loadings. (source: by authors)

This behavior suggests that *g-C_3N_4* incorporation enhances microbial electron transfer at moderate loading, while excessive incorporation disrupts conductive pathways within the carbon matrix. The superior performance at 5 wt%, therefore, reflects a more favorable internal distribution of g-C_3N_4 that supports both microbial activity and electron flow.

3.3. Evaluation of the impact of g-C3N4 on the power density

Figure 6 and Figure 7 show the electrochemical performance of the MFC with g-C_3N_4 added to the anodes at different percentages (5, 10, and 12 wt%). Figure 6 shows the change over time of the maximum power density measured every 2 days starting on day 8 of installation. Across all metrics, the 5 wt% g-C_3N_4 anode exhibited superior performance. Notably, on day 14, the maximum power density reached 43.245 μW/cm², approximately 1.9 times higher than the 23.256 μW/cm² of the anode without addition. In the power density curve, the 5 wt% addition condition also showed a significant increase in power output relative to current density compared to the other conditions, confirming that it has excellent energy conversion efficiency. These results suggest that the moderate addition of g-C_3N_4 (5 wt%) effectively promotes microbial activity and electron transfer on the anode surface and improves MFC performance. On the other hand, higher additions (10 wt% and 12 wt%) tended to suppress performance, suggesting that excess g-C_3N_4 may adversely affect electron transfer and microbial activity.

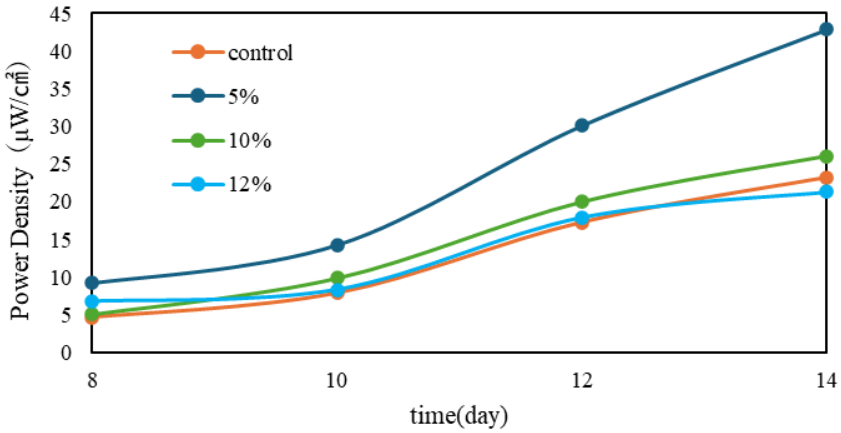

Figure 6: Maximum power density versus g-C_3N_4 addition and number of days.(source: by authors)

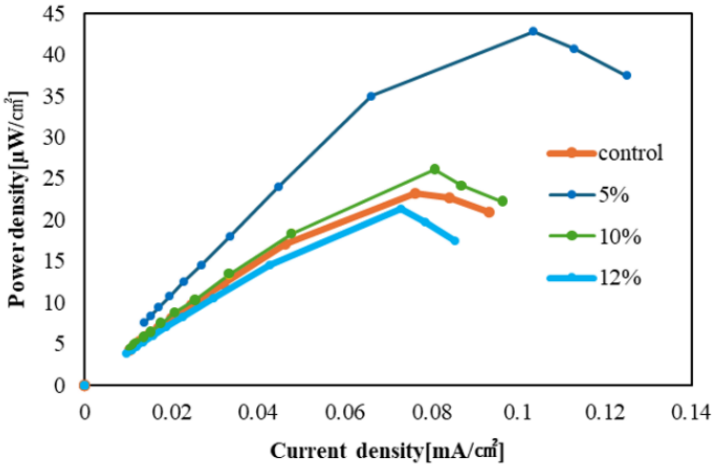

Figure 7 Power density curves on day 14 with varying g-C_3N_4 content. (source: by authors)

As shown in Figure 7, the anode containing 5 wt% g-C_3N_4 exhibits the highest power density over the entire current density range.This result suggests that moderate g-C_3N_4 incorporation provides a favorable balance between enhanced microbial activity and sufficient electrical conductivity, whereas excessive loading negatively affects electron transport

These results indicate that the performance trend is governed by how *g-C_3N_4* incorporation modifies the internal electron pathways and microbial attachment sites. At 5 wt%, g-C_3N_4 is sufficiently integrated to enhance biofilm formation and electron transport, whereas higher loadings disrupt conductivity and reduce efficiency. The observed performance differences can therefore be interpreted based solely on how *g-C_3N_4* incorporation affects internal conductivity and microbial colonization. This explanation strengthens the validity of the case study without requiring additional experiments or simulations. This study provides a clear framework for understanding how nitrogen-rich additives influence both the biological and conductive properties of carbonaceous anodes. By presenting a comparative evaluation based solely on controlled loading variations, the work offers insights that are broadly applicable to the design of future biomass-derived MFC electrodes.

4. Conclusion

This study demonstrated that embedding graphitic carbon nitride (g-C_3N_4) into rice-husk-derived biochar significantly enhances microbial fuel cell performance through improved electron transfer and biofilm development. Among the tested loading amounts, 5 wt% g-C_3N_4 produced the most favorable electrochemical behavior, achieving a power density nearly 1.9 times higher than the unmodified anode and exhibiting the most stable anode potential. These findings reveal the importance of balancing nitrogen-induced microbial activity with the electrical conductivity of the carbon matrix. The results confirm that g-C_3N_4-embedded biochar represents a practical, low-cost, and environmentally sustainable anode material. Future research should focus on elucidating the detailed mechanisms of microbe–g-C_3N_4 interactions, optimizing structural properties, and evaluating long-term performance in real wastewater environments.

Future studies should investigate the long-term stability of g-C_3N_4-embedded anodes under fluctuating environmental conditions and continuous-flow MFC systems. Structural optimization of pore size distribution, nitrogen content, and surface functionalization may further enhance microbial electron transfer efficiency. Additionally, metagenomic analysis of the microbial community would provide insights into how g-C_3N_4 influences microbial composition and metabolic pathways. Scaling-up experiments and cost evaluations will also be essential to assess the feasibility of practical applications in wastewater treatment systems.

Acknowledgements

The abstract of this paper was presented at the Green Urbanism (GU) Conference-9th Edition, which was held on the 25th – 27th of November 2025.

Funding declaration

This research did not receive any specific grant from funding agencies in the public, commercial, or not-for-profit sectors/individuals.

Ethics approval

Not applicable.

Conflict of interest:

The author(s) declare that there is no competing interest

References

Hirose, S., Nguyen, T. D., & Taguchi, K. (2023).Development of low-cost block-shaped anodes for practical soil microbial fuel cells. *Energy Reports, 9* (3), 144–150.

Jian, M., Xue, P., Zhang, X., Xing, Y., Ma, L., Lv, X., & Shi, K. (2024).Enhanced performance of acridine degradation and power generation by microbial fuel cells with g-C_3N_4/PANI-DA/CF anodes. *Chemosphere, 362*, 141752. https://doi.org/10.1016/j.chemosphere.2024.141752

Li, W.-W., Sheng, G.-P., Liu, X.-W., & Yu, H.-Q. (2011).Recent advances in the separators for microbial fuel cells. *Bioresource Technology, 102*, 244–252.

Logan, B. E., Hamelers, B., Rozendal, R., Schröder, U., Keller, J., Freguia, S., Aelterman, P., Verstraete, W., & Rabaey, K. (2006). Microbial fuel cells: Methodology and technology. *Environmental Science & Technology, 40*(17), 5181–5192. https://doi.org/10.1021/es0605016

Mishra, A., Mehta, A., Basu, S., Shetti, N. P., Reddy, K. R., & Aminabhavi, T. M. (2019).Graphitic carbon nitride (g-C_3N_4)-based metal-free photocatalysts for water splitting: A review. *Carbon, 149*, 693–721. https://doi.org/10.1016/j.carbon.2019.04.104

Mishra, A., Mehta, A., Kainth, S., & Basu, S. (2018). A comparative study on the effect of different precursors for the synthesis and efficient photocatalytic activity of g-C_3N_4/TiO_2/bentonite nanocomposites. *Journal of Materials Science, 53*, 13126–13142. https://doi.org/10.1007/s10853-018-2565-0

Pant, D., Van Bogaert, G., Diels, L., & Vanbroekhoven, K. (2010). A review of the substrates used in microbial fuel cells (MFCs) for sustainable energy production. *Bioresource Technology, 101*, 1533–1543. https://doi.org/10.1016/j.biortech.2009.10.017

Sayed, E. T., & Nakagawa, N. (2017). Critical issues in the performance of yeast-based microbial fuel cells. *Journal of Chemical Technology & Biotechnology, 93* (6), 1588–1594. https://doi.org/10.1002/jctb.5527

Sayed, E. T., Abdelkareem, M. A., Alawadhi, H., Elsaid, K., Wilberforce, T., & Olabi, A. G. (2021).Graphitic carbon nitride/carbon brush composite as a novel anode for yeast-based microbial fuel cells. *Energy, 221*, 119849. https://doi.org/10.1016/j.energy.2021.119849

Sayed, E. T., Shehata, N., Abdelkareem, M. A., & Atieh, M. A. (2020). Recent progress in environmentally friendly bio-electrochemical devices for simultaneous water desalination and wastewater treatment. *Science of the Total Environment*, 748, 141046. https://doi.org/10.7748/phc.2016.e1162

Yan, S. C., Li, Z. S., & Zou, Z. G. (2009). Photodegradation performance of g-C_3N_4 fabricated by directly heating melamine. *Langmuir, 25*(17), 10397–10401. https://doi.org/10.1021/la900923z